DETAILED MODELLING OF THE EFFECTIVE MINORITY CARRIER LIFETIME AND THE OPEN-CIRCUIT VOLTAGE OF SILICON SOLAR CELLS

Andres Cuevas[1] and Ronald A. Sinton[2]
[1]Department of Engineering, Australian National University, Canberra, ACT 0200, Australia
[2] Sinton Consulting, Boulder, CO, USA

ABSTRACT: The effective lifetime of minority carriers within a silicon wafer under varying illumination can be easily measured using a quasi-steady state photoconductance (QSSPC) instrument. Similarly, the open-circuit voltage of a solar cell precursor can be tested as a function of light intensity using the Suns-V_{oc} method. Because of their inherent ability to scan a broad range of carrier injection levels both techniques are very well adapted to investigate silicon materials and solar cells. Often, however, the carrier density profile is non-uniform and this creates a large source of uncertainty in the analysis of the lifetime or voltage data. This paper presents a comprehensive computer model capable of determining the excess carrier density profile for arbitrary recombination rates, photon absorption, illumination intensity and temperature. Through detailed modelling, it is possible to reveal the hidden complexities of the effective lifetime and the open-circuit voltage and draw meaningful conclusions from measured data.
Keywords: lifetime, modelling, silicon.

1 INTRODUCTION

In the last thirteen years, since the first hand crafted testers came out of the Sinton atelier [1], QSS photoconductance instruments have become pandemic among silicon solar cell labs. While they have greatly simplified the measurement of the effective carrier lifetime, analysing the results may be difficult, due to the complex physics that match recombination to photogeneration in a silicon wafer. To assist with the analysis and thus exploit the potential of QSSPC measurements, it is necessary to complement the experiment with theoretical modelling.

Although computer programs, such as PC1D [2], are available to model silicon wafers and devices, there is still a need for a model specifically adapted to the QSSPC [3] and Suns-V_{oc} [4] techniques. This paper presents a spreadsheet implementation that we have capriciously called QSS-Model, despite the fact that it is restricted to steady state and open-circuit conditions. The model solves the equations describing carrier transport and recombination in the semiconductor for an arbitrary injection level, while using injection dependent and position dependent material parameters. Mathematical details are given in the Appendix.

QSS-Model can be used to study the injection dependence of the different recombination mechanisms that coexist within the wafer, in order to differentiate one from another. Temperature dependences can also be explored, Suns-V_{oc} curves can be plotted and ideal fill factors can be determined. The results are presented in a form that can be directly compared to the experimental data from lifetime or open-circuit voltage measurements. Such use of modelling enables the efficient design of experiments for process control and device optimization by anticipating the sensitivity of measurement tools to determine the parameters of interest.

2 THE EFFECTIVE LIFETIME

2.1 The concept of effective lifetime revisited

Silicon wafers can conceal beneath their opaque appearance several different layers, such as dopant diffusions, quasi-neutral base regions and space-charge regions. The destiny of electrons and holes is to perish (the wafer is in open-circuit, so they are confined between the two surfaces of the wafer) and, as soon as they are generated by light, they seek a place that gives them a quick death. In multicrystalline silicon they may even travel across boundaries to reach grains that offer a faster recombination service.

Diverse and colourful as it may be, the world of electrons and holes is well represented by the average electron (or hole, if you prefer) and by the concept of *effective* lifetime, τ_{eff}. This simply is the time the average electron lives in the wafer. Irrespective of whether it happens predominantly in the bulk, or at the surfaces, the global recombination rate in the wafer can be expressed as:

$$R_{Total} = \frac{\Delta n_{av} W}{\tau_{eff}} \qquad (1)$$

where Δn_{av} is the average excess carrier density in the wafer and W its thickness. In its simplest interpretation, this definition of τ_{eff} intuitively reflects a simple case where the excess carrier density would be uniform, that is $\Delta n(x)=\Delta n_{av}$, and recombination would take place exclusively in the base region via a mechanism that could be well described by a constant minority carrier lifetime, $\tau_n=\tau_{eff}$. Such cases do exist, for example when the surfaces of the wafer are well passivated and the minority carrier diffusion length is larger than the wafer thickness, or when the photogeneration that creates the excess carriers is approximately uniform (and surface recombination is still negligible).

In practice, however, there are many instances when the excess carrier density varies with position, the lifetime is a function of the carrier density itself, and there are several recombination mechanisms competing for the annihilation of electrons and holes. The concept of effective lifetime can still be used to describe such cases, but it is necessary to remember that it may then give an oversimplified picture of the physical reality. This is where theoretical modelling comes into play, to

help understand the physics and extract as much information as possible from the measured τ_{eff}. Which brings us to the measurement technique itself.

2.2 The robustness of the QSSPC technique

When measuring the excess photoconductance, what we actually determine is an integrated excess carrier density, as described by the following expression:

$$\Delta\sigma_{\mathrm{L}} = q\int_0^W \left(\mu_n(x)+\mu_p(x)\right)\Delta n(x)\mathrm{d}x \qquad (2)$$

The conductance of the wafer may be composed of several contributions from different layers, but the largest and most important is the conductance of the quasi-neutral region (sometimes called the base) that typically occupies most of the wafer. In extreme cases even very thin layers, such as space-charge regions created by pn junctions or charged dielectrics, cannot be ignored. Nevertheless, QSS-Model does ignore them to focus on the quasi-neutral region. Of course, the hardware measures everything that may contribute to the photoconductance, even if such contributions may be unrelated to recombination, as is the case when depletion region modulation [5] or minority carrier trapping [6] are significant. In summary, the hardware measures τ_{eff}, the lifetime of an electron in the sample under the conditions that it is being tested. For example, if the electron is photogenerated near an unpassivated surface, this lifetime is short. If the wafer is perfectly passivated, then $\tau_{eff}=\tau_{bulk}$.

In the experiment the exact shape of the excess carrier density profile remains unknown. This does not matter much if all we want to do is find the effective lifetime, noting that the electron and hole mobilities do not usually change much as a function of position within the wafer. Then we can write the excess photoconductance as:

$$\Delta\sigma_{\mathrm{L}} \approx qW\left(\mu_n+\mu_p\right)\Delta n_{av} \qquad (3)$$

which immediately leads to the effective lifetime:

$$\tau_{eff} = \frac{\Delta\sigma_{\mathrm{L}}}{q\left(\mu_n+\mu_p\right)G_{\mathrm{Total}}} \qquad (4)$$

where we have used the balance between total recombination and generation that characterises the steady state and replaced R_{total} with G_{total}, which can be easily measured.

The mobilities of electrons and holes to use in Eqns. 3 and 4 are the *conductivity* mobilities, which are well characterised, for example by Danhauser and Krause [7]. They are approximately constant up to an excess carrier density of about $10^{16}\mathrm{cm}^{-3}$, which is convenient for the simplified derivations made above. The problem is that QSSPC hardware can easily produce excess carrier densities well above that value and then the conductivity mobilities are a decreasing function of the carrier density itself. Both the hardware and QSS-Model deal with this by selecting the value of $\mu_n+\mu_p$ that corresponds to the particular Δn_{av} being measured (a couple of iterations suffice). This procedure makes the experimental determination of τ_{eff} quite robust.

The theoretical model does determine the excess carrier profile, $\Delta n(x)$, and therefore it would be possible to calculate its average value mathematically, for example as the arithmetic mean. Nevertheless, the photoconductance based Δn_{av}, defined by Eq. 3, is more useful to make comparisons between theory and experiment. QSS-Model replicates the experiment by first calculating the photoconductance as per Eq. 2, where $\mu_n(x)+\mu_p(x)$ is a function of position, and then using Eq. 3 iteratively to find the single value of $\mu_n+\mu_p$ that corresponds to the particular Δn_{av}.

3 EXAMPLES OF APPLICATION OF QSS-MODEL

3.1 An example of nearly constant lifetime

By balancing generation and recombination the model allows us to determine τ_{eff}, in fact, not just τ_{eff} but also Δn_{av} over a broad range of Δn_{av}. So naturally we should plot τ_{eff} as a function of Δn_{av} to imitate what the QSSPC hardware does. Other experimental techniques such as Suns-V_{oc} or photoluminescence may be used to access even lower values of Δn_{av}. Two examples of τ_{eff} vs. Δn_{av} are shown in Fig. 1, not measured of course, but generated with the model, given the nature of this paper.

The first example is a common 1.5Ωcm p-type silicon wafer that happens to contain a fairly large, but not unusual in mc-Si, concentration of iron, $[\mathrm{Fe}]=1\mathrm{x}10^{12}\mathrm{cm}^{-3}$. If the wafer is measured after having been in the dark for a few hours, the iron is paired with boron, which creates a specific recombination centre that results in a nearly constant lifetime of about 14.5µs in this case. Experts in the physics of Shockley-Read-Hall recombination would explain this constant lifetime by pointing out that the capture cross sections for electrons and holes for the FeB recombination centre are very similar [8].

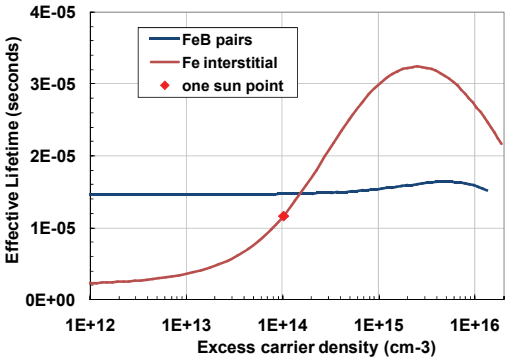

Figure 1. Effective lifetime as a function of the average excess carrier density for a 1.5Ωcm p-type silicon wafer having $10^{12}\mathrm{cm}^{-3}$ recombination centres of either interstitial iron or FeB pairs. Surface recombination is typical of a BSF silicon solar cell.

When the lifetime is constant our job is relatively easy: we can report just one value (14.5µs) and calculate the corresponding diffusion length for electrons (235µm), which happens to be close to the wafer thickness (250µm). So one would think that this is not a bad quality wafer, since most carriers will be collected at the front junction when placed in short-circuit. The current in short-circuit could be calculated using more sophisticated software, such as PC-1D, or perhaps some hyper-long hyperbolic mathematical expressions. In actual fact, this is not such a great quality wafer, because a lifetime of

14.5µs means that the recombination *rate* in open-circuit, when the excess carrier density is highest, will be high and hence the voltage relatively low. We will explore the open-circuit voltage later.

3.2 An example of strongly varying lifetime

If we now subject the 1.5Ωcm p-type iron contaminated ([Fe]=1x10^{12}cm^{-3}) silicon wafer to strong illumination for a few minutes, the iron-boron pairs dissociate and interstitial iron becomes the dominant recombination centre. The result is a lifetime that varies strongly with injection level, as can be seen in Fig.1. This strong variability of the SRH lifetime is due to very asymmetric capture cross sections for electrons and holes in the case of Fe_i [8]. The change in lifetime behaviour after illumination is a distinctive signature of iron, with a well-defined cross-over between the two lifetime curves at an excess carrier density of Δn=1.72x10^{14}cm^{-3} [9].

Obviously, it is now difficult to characterise the wafer with a single lifetime value. At low injection levels, τ_n=2.5µs, the diffusion length is L_n=8.3µm and the carrier density profile is almost exponential, ten times higher at the front than at the rear (see Fig.2). For an illumination of 10 suns the *effective* lifetime reaches a maximum of τ_{eff}=32.5µs. Note that we do not dare to identify this with the bulk lifetime, given that the *effective* diffusion length that corresponds to such lifetime is L_{eff}=313µm, greater than the wafer thickness, in which case the effects of the rear surface may be important. The model reveals that indeed, 72% of the total recombination now occurs at the back surface, and 15% at the front. The corresponding carrier profile is practically a straight line, indicating that there is almost no bulk recombination (see Fig.3). Therefore, the effective lifetime of τ_{eff}=32.5µs is mostly a representation of rear surface recombination, which is the dominant loss in this modelled BSF solar cell at ten suns.

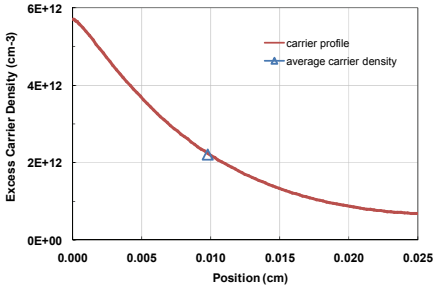

Figure 2. Excess carrier density profile at 0.1 suns for a 1.5Ωcm p-type, 250µm thick silicon wafer with interstitial iron. The diffusion length is L_n=8.7µm.

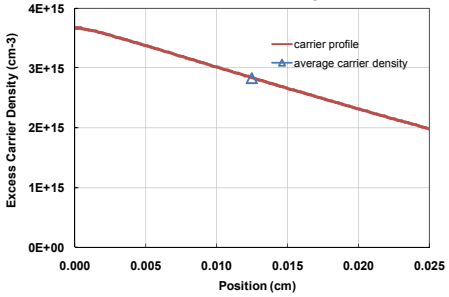

Figure 3. Excess carrier density profile in the same wafer of Fig.2 at 10 suns. The diffusion length is L_n=890µm.

3.3 The importance of passivating the surfaces

The true bulk lifetime and diffusion length in the previous example could only be seen if surface passivation was improved. This is easier to do in theory than in practice. With zero surface recombination the model gives the result shown in Fig. 4, where the lifetime, now identifiable with the true minority carrier lifetime reaches a maximum value of τ_n=400µs. At 0.1 suns, however, the lifetime is still τ_n=2.6µs; therefore, the SRH lifetime characteristic of Fe_i spans approximately a factor of 150. As a result, the carrier density profile varies, for the case of white light discussed so far, from a nearly exponential shape (as shown in Fig. 2) to being constant (there is no rear surface recombination now). Clearly, it would be better to always have a flat carrier profile to interpret injection-dependent lifetime measurements more easily. One possibility is to use weakly absorbed light, selecting a wavelength of 1100nm. Two different calculations, using either the AM1.5G spectrum or 1100nm infrared light, gave essentially the same shape for the τ_{eff} vs. Δn_{av} curve in this case. Nevertheless, increasing the iron concentration lowers the lifetime and makes the result more sensitive to the spectrum of illumination.

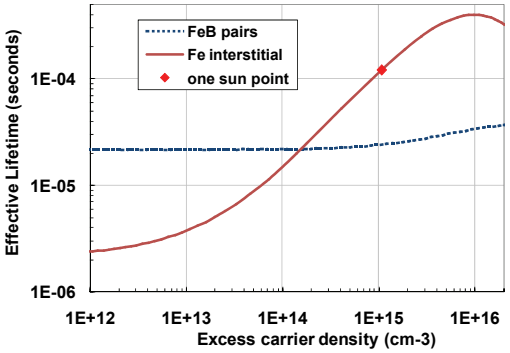

Figure 4. Lifetime fingerprint of iron ([Fe]=10^{12}cm^{-3}) on a 1.5Ωcm p-type silicon wafer. No surface recombination. AM1.5G spectrum.

The spectrum of the illumination used in the QSSPC experiment can have a significant impact on the resulting τ_{eff}. QSS-Model permits to choose among several spectra, as well as monochromatic illumination. A classical case where the use of infrared illumination is highly beneficial is when the surfaces have a very high recombination velocity, as is the case in unprocessed wafers. Table I shows the lifetimes that would be measured at an excess carrier density of Δn=10^{13}cm^{-3} using either the unfiltered spectrum of the xenon flash used in QSSPC hardware, or the flash plus a filter that passes all wavelengths higher than 750nm, or a monochromatic light of 1100nm that creates a uniform photogeneration within the wafer. The cases of interstitial iron, FeB pairs and, for reference, an uncontaminated wafer, are shown. The highest effective lifetime that could be expected in this case is τ_{eff}=1.74µs, even in a wafer with high bulk lifetime.

An interesting question to ask is whether it may be possible to measure iron contamination in an unprocessed wafer, using for example the flash plus IR filter. The τ_{eff} vs. Δn_{av} curves in Fig. 5 give the answer: yes, if the lifetime can be measured with sufficient accuracy, which is normally possible with the QSSPC technique,

particularly because only a relative change in lifetime is needed to determine the concentration of iron. Note that the cross-over point is still the same as in Figs. 1 and 4. It is obvious in Fig. 5 that the measurement of iron can only be taken below the cross-over point, that is, at low illumination intensities. Practical difficulties such as trapping could hinder the measurement, and it would be preferable to use thicker wafers so that the measurable lifetimes are higher, or perform the measurement on the silicon ingot, as demonstrated in [10]. Doing the measurement at a higher temperature may also help.

Spectrum	τ_{eff} (Fe int.) (µs)	τ_{eff} (FeB) (µs)	τ_{eff} (max) (µs)
Flash	0.42	0.58	0.64
Flash+filter	0.65	0.9	1
1100nm	1.12	1.57	1.74

Table I. Effective lifetime at Δn=10^{13}cm^{-3} for a 250µm thick, 1.5Ωcm p-type unpassivated Si wafer using different illumination spectra.

There is a trend in the τ_{eff} curves of Fig. 5 to keep increasing with carrier density. This is not because of the injection dependence of the iron-dominated bulk lifetime (the same trend is observed in an uncontaminated wafer), but is due to the finite diffusion velocity of electrons and holes, which results in a slight change in the shape of the carrier density profile at high current densities, as a crowd of carriers flows towards the surfaces.

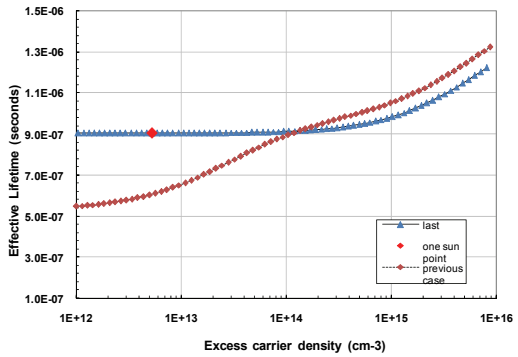

Figure 5. Lifetime fingerprint of iron ([Fe]=10^{12}cm^{-3}) on a 1.5Ωcm p-type silicon wafer when surface recombination is extremely high. Flash spectrum with a 750nm IR pass filter.

4 ILLUMINATION INTENSITY VS. OPEN-CIRCUIT VOLTAGE CURVES

4.1 Implied and actual voltages (the case of FeB pairs)

After having stressed the importance of the surfaces, we can now mention that, in QSS-Model, we have characterised surface recombination by means of a saturation current density, a concept that will hopefully become clearer in this section. Let us come back to the example discussed in section 3.1, which is meant to represent an industrial BSF silicon solar cell, with a phosphorus diffusion at the front and an aluminium-doped p^+ region at the rear. Typical values that characterise these two regions as produced by common industrial technology are $J_{o(front)}$=10^{-13}Acm^{-2} and $J_{o(back)}$=10^{-12}Acm^{-2}, respectively. In QSS-Model the two surface regions have zero thickness, that is, they are idealised boundary conditions for the quasi-neutral base region. Aspects related to photons absorbed in the front diffusion, which may not contribute to creating excess carriers in the base if recombination in that diffused region is very strong, are not included. Space-charge regions are also left out of the model.

After having modelled or measured the effective lifetime, we realise that, after all, if there are carriers in excess over their equilibrium concentrations, as is the case in the photoconductance experiment, there must also be a voltage (physicists express this as a separation between the quasi-Fermi levels for electrons and holes). So we go ahead and calculate the implied V_{oc} using our knowledge of the dopant density and Δn_{av} corresponding to one sun (AM1.5G) illumination, obtaining in the case of FeB pairs $V_{oc(implied)}$=604mV.

The expression that we should have used is

$$\Delta n(0)[N_A + \Delta n(0)] = n_i^2 \exp\left(\frac{V_{oc}}{kT/q}\right) \qquad (5)$$

but instead of the excess minority carrier density at the junction edge of the quasi-neutral base region, $\Delta n(0)$, we have used Δn_{av}, which may lead to errors in the evaluation of V_{oc} [11]. Using QSS-Model we find that the actual device voltage at one sun illumination should be slightly higher, V_{oc}=612mV. In the case of FeB pairs the diffusion length is nearly equal to the wafer thickness and the carrier density does not vary drastically with position. Nevertheless, the small difference between $\Delta n(0)$=1.8x10^{14}cm^{-3} and Δn_{av}=1.3x10^{14}cm^{-3} explains the 8mV discrepancy between V_{oc} and $V_{oc(implied)}$.

Only laziness could keep us from plotting all the values of V_{oc} that can be calculated as a function of light intensity, which, with a small conceptual effort, we can visualize as a photogenerated current density, J_{ph}. Admittedly, it may be quicker to directly measure the actual V_{oc} and obtain the Suns-V_{oc} curve [4]. The modelled V_{oc} as a function of J_{ph} for the case of FeB pairs gives a straight line in the semi-logarithmic plot of Fig. 6, which is, not surprisingly, as featureless as the corresponding lifetime curve.

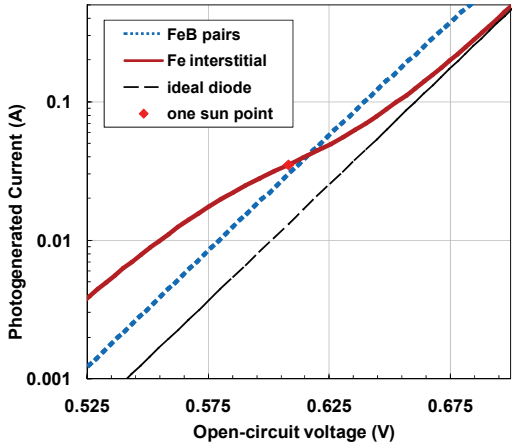

Figure 6. Suns-V_{oc} curves (converted to photogenerated current) for a 1.5Ωcm silicon wafer contaminated with iron ([Fe]=10^{12}cm^{-3}). For comparison, an ideal diode curve (n=1) is also shown.

The J_{ph}-V_{oc} characteristic curve for FeB pairs in Fig. 6 would quickly be interpreted by device engineers as following Shockley's ideal diode equation:

$$J_{ph} = J_0 \exp\left(\frac{V_{oc}}{nkT/q}\right) \qquad (6)$$

with an *ideality factor* equal to one (which precisely constitutes the definition of ideal diode) and a saturation current density of J_o=1.8x10^{-12}Acm^{-2}.

Comparing the sum $J_{o(front)}$+$J_{o(back)}$=1.1x10^{-12}Acm^{-2} to the total J_o=1.8x10^{-12}Acm^{-2} obtained from the ideal diode fit we can understand that this global J_o includes not only the surfaces, but also the bulk, that is, it reflects the total recombination in the device, in much the same way as τ_{eff} does. QSS-Model can show that, in this case, the cumulative recombination across the wafer mostly occurs in the base region, rather than at the surfaces.

We can take our analysis one step further by shifting the J_{ph}-V_{oc} data and re-plotting them as a photovoltaic curve [4], from which we could calculate an ideal fill factor FF=0.83.

4.2 Suns-V_{oc} characteristics for interstitial iron

The shape of the J_{ph}-V_{oc} curve for the case dominated by interstitial iron, shown in Fig.6, presents a clear departure from the ideal diode equation. It is no longer possible to fit it using a single value of J_o. The local ideality factor can, nevertheless, be calculated for every voltage point using Eq. 6, and the result is plotted in Fig. 7. It can be seen that the strong variability of the lifetime in Fig. 1 results in ideality factors that may traditionally have been attributed to space charge recombination, when in reality they are still a manifestation of recombination in the bulk, quasi-neutral region of the wafer [12]. The analysis of the Suns-V_{oc} data as a photovoltaic curve gives an ideal fill factor FF=0.786, much lower than for the case of FeB pairs. The open-circuit voltage at one sun would now be 608mV.

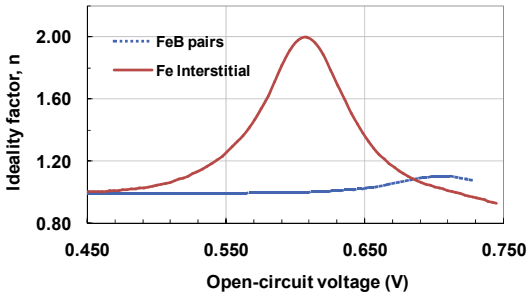

Figure 7. Local ideality factors corresponding to the Suns-V_{oc} curves in Fig. 6.

The implied voltage for a Fe_i dominated device (not shown) is much lower than the actual voltage at low illumination levels, when the minority carrier profile decreases strongly with position due to L_n<<W. As explained above, the reason for the difference between the implied and actual voltages lies in the specific shape of the carrier density profile, $\Delta n(x)$. In this case it is shown in Fig. 2: at 0.1 suns, Δn_{av}=2.2x10^{12}cm^{-3} is considerably smaller than $\Delta n(0)$=5.7x10^{12}cm^{-3} and $V_{oc(implied)}$=498mV is much smaller than V_{oc}=523mV. A manual correction in the evaluation of $V_{oc(implied)}$ could me made [11], but the fact remains that the evaluation of the voltage from photoconductance can be misleading if not done carefully. Modelling is recommended in such cases.

The experimental methods for the QSS-V_{oc} technique are very simple. Suns-V_{oc} curves can be taken before or after final cell metallisation. The two curves shown in Fig.6 for the cases of interstitial iron and FeB pairs have an interesting message: there is a voltage point where they cross each other, V_{oc}=615mV. This may be used to detect iron at the device level. What usually happens is that, once the phosphorus diffusion has been performed, the concentration of interstitial iron drops drastically due to gettering (down to [Fe_i]=10^{11}cm^{-3} or less), and its detection would require a device with a better rear surface passivation.

5 TEMPERATURE DEPENDENT LIFETIME

Similarly to injection-dependent measurements, temperature-dependent lifetimes, although not as easy to implement experimentally, have become a useful tool for the spectroscopic determination of the fundamental recombination parameters of SRH recombination centres. In our case the process is the opposite: we use published data for those parameters and calculate what the temperature dependence of the lifetime can be expected to be. An example is shown in Figure 8, again for iron in p-type silicon. Temperature affects the voltage of solar cells, as everybody knows. For example, the Suns-Voc curve for interstitial Fe calculated at 100 ^{o}C indicates that the fill factor would be 0.71, well below the value of 0.786 at 27^{o}C.

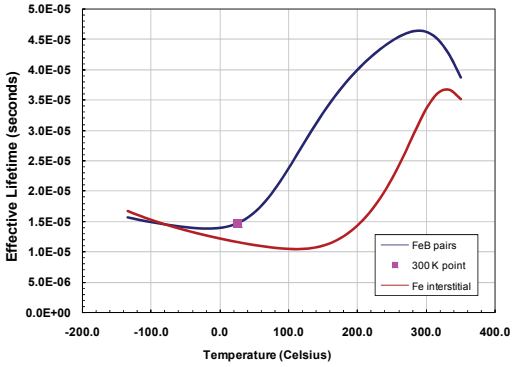

Figure 8. Modelled temperature dependent lifetime for an FeB pairs and for interstitial iron ([Fe]=1x10^{12}cm^{-3}) in an 1.5Ωcm silicon wafer at one sun illumination.

6 CONCLUSIONS

QSS-Model is a useful complement to QSSPC and Suns-V_{oc} hardware. Although in most cases the effective lifetime is a sufficiently meaningful parameter, its de-convolution into separate recombination mechanisms must be done with care. Modelling the experimental situation helps to understand the limitations of the simple, first-order analysis, and fine tune it when necessary. The possibility of visualising injection and temperature dependences of the effective lifetime, combined with their translation into Suns-V_{oc} characteristic curves permits to establish direct links between specific defects or metal impurities and device

parameters such as V_{oc}, FF and ideality factor.

QSS-Model can be freely downloaded from: http://engnet.anu.edu.au/DEresearch/semiconductor.

APPENDIX. Basic equations for determining the excess carrier density

The global balance between generation and recombination, for a wafer in open-circuit, does not exclude the possibility of internal flows of electrons and holes within the wafer. If we consider a small volume defined by an interval of distance, Δx, the concentration of carriers can increase due to the injection of electrons into that volume, $-J_n$, or to the photogeneration occurring within it, G_L. The two mechanisms that can make it decrease are the current that leaves the slice of material, $J_n(x+\Delta x)$, and recombination within it, defined by R_v, the volume recombination rate. We can, therefore, write

$$-J_{\mathrm{n}}(x+\Delta x) = -J_{\mathrm{n}}(x) + qG_L(x)\Delta x - qR_{\mathrm{v}}(x)\Delta x \qquad \text{(A1)}$$

This equation represents, when the element size is infinitesimally small, the integral form of the continuity equation. In addition, the transport equations relate the carrier density to the electron current. Open-circuit, zero total current conditions imply that the electron and hole currents are identical

$$J_{\mathrm{n}}(x) = -J_{\mathrm{p}}(x) \qquad \text{(A2)}$$

In general, the current is made up of a diffusion term and a drift term. Both can be lumped together into an effective diffusion coefficient, D_{eff}:

$$D_{eff} = \frac{(n+p)D_nD_p}{nD_n + pD_p} \qquad \text{(A3)}$$

The electron current can thus be expressed as:

$$J_{\mathrm{n}}(x) = qD_{eff}\frac{dn}{dx} \qquad \text{(A4)}$$

or, in integral form, considering a small interval, so that the current can be considered approximately constant within it:

$$\Delta n(x+\Delta x) = \Delta n(x) + \frac{J_{\mathrm{n}}(x)}{qD_{eff}}\Delta x \qquad \text{(A5)}$$

This equation permits to find the electron concentration as a function of position, with the electron current being determined from Eq. A1. Note that D_{eff} is, in general, injection level dependent and also position dependent. In addition the electron and hole diffusion coefficients, D_n and D_p can be themselves injection level dependent.

In deriving these equations, valid for any injection level and dopant densities, the only assumptions have been that departures from charge neutrality are very small (hence the name quasi-neutral region), so that $\Delta n=\Delta p$ (note that this is also necessary for the applicability of the SRH recombination model), and $d\Delta n/dx=d\Delta p/dx$. Both conditions are usually met in the semiconductor.

The boundary conditions that the carrier density profile must satisfy come from the fact that the rate at which carriers flow towards the surface must be equal to the rate at which they recombine there. The latter can be expressed by means of a saturation current density:

$$R_{front\ surf} = J_{0\mathrm{front}}\frac{p_{front}n_{front} - n_i^2}{qn_i^2} \qquad \text{(A6)}$$

If desired, the minority carrier surface recombination velocity can be found from its definition:

$$S_{\mathrm{n}} = S_{\mathrm{p}} \equiv \frac{R_{surf}}{\Delta n_{surf}} \qquad \text{(A7)}$$

In our model the surfaces have zero thickness and space charge regions have not been included. The full Shockley-Read-Hall bulk recombination model has been implemented, with up to date values for the energy levels and capture cross sections of the most important metal impurities, as well as for the B-O complex in CZ silicon. Intrinsic Auger and band to band recombination has been implemented using the empirical expression proposed by Kerr et al.

As a consequence of the different mobilities of electrons and holes, an electric field may develop within the wafer to assist the flow of the latter and help maintain charge neutrality. The consequence of this is an electrostatic potential drop across the base region, V_{Base}. This *Dember effect* voltage is only significant for lowly doped silicon when the carrier profile is highly non-uniform. Note that if the position of the n^+ and p^+ regions is reversed (that is, p^+ at the front, illuminated face), the expression for the voltage is slightly different. Finally, the open-circuit voltage of an n^+pp^+ solar cell structure can be determined as:

$$V_{oc} = \frac{kT}{q}\ln\left(\frac{(n_o + \Delta n_{front})(p_o + \Delta n_{back})}{n_i^2}\right) + V_{Base} \qquad \text{(A8)}$$

Acknowledgments

We are indebted to D. Macdonald, E. Franklin, K. Macintosh, K. Bothe and S. Bowden for assisting in the development of the QSS-Model spreadsheet implementation and providing useful data. A.C. acknowledges continuous support from the Australian Research Council.

References

[1] R. A. Sinton, NREL Workshop, 1995.

[2] D. A. Clugston and P. Basore, 26th IEEE Photovoltaic Specialists Conf., Anaheim CA, pp. 207-210, 1997.

[3] R. A. Sinton and A. Cuevas, *Appl. Phys.Lett*., Vol. 69(17), p. 2510 (1996).

[4] R. Sinton and A. Cuevas, *Proc. 16th European Photovoltaic Solar Energy Conf.*, Glasgow, May 2000, pp.1152-1155.

[5] M.Bail, M.Schulz and R.Brendel, *Appl. Phys. Lett*. 82, 757 (2003).

[6] D. Macdonald and A. Cuevas, *Appl. Phys. Lett*. 74, 1710 (1999).

[7] F. Danhaüser, *Solid-St. Electron* 15, 1371 (1972), and J. Krausse, *Solid-St. Electron* 15, 1477 (1972).

[8] D. Macdonald, A. Cuevas and J. Wong-Leung, *J. Applied Physics* **89**(12), p. 7932 (2001).

[9] D. Macdonald, T. Roth, P. N. K. Deenapanray, T. Trupke and R. A. Bardos, Appl. Phys. Lett. 89, 142107 (2006).

[10] R. A. Sinton, T. Mankad, S. Bowden, and N. Enjalbert, *19th European Photovoltaic Solar Energy Conf.,* 2004.

[11] A. Cuevas and R. Sinton, *Progress in Photovoltaics*, Vol 5, pp 79-90 (1997).

[12] D. Macdonald and A. Cuevas, *Prog. Photovolt: Res. Appl.* **8**(4), 363-375 (2000).